Journal of Rock Mechanics and Geotechnical Engineering. 2010, 2 (2): 149–154

Journal of Rock Mechanics and Geotechnical Engineering

Journal online: www.rockgeotech.org

# Unsaturated creep tests and empirical models for sliding zone soils of Qianjiangping landslide in the Three Gorges

Xiaoling Lai*, Shimei Wang, Hongbin Qin, Xianfeng Liu

*Key Laboratory of Geological Hazards in Three Gorges Reservoir Area, Ministry of Education, China Three Gorges University, Yichang, 443002, China*

*Received 23 August 2009; received in revised form 10 October 2009; accepted 25 October 2009*

**Abstract:** Creep of sliding zone soils may cause significant displacement in large-scale landslides in the Three Gorges reservoir area. To investigate the effects of water on the soil creep behavior of the Qianjiangping landslide, a series of unsaturated triaxial creep tests on the sliding zone soils were performed. Based on the analyses of testing results, a new stress intensity incorporating matric suction was defined and an unsaturated Singh-Mitchell creep model was developed. Predicted results are in good agreement with the experimental results, which indicates that the established unsaturated model can reasonably simulate the effects of water on the soil creep behavior of the landslide. Finally, relationships between matric suction and the parameters of the model were analyzed. This study provides a calculation model and parameters for the evaluation of long-term stability of landslides under the influence of water.

**Key words:** Qianjiangping landslide; matric suction; creep; Singh-Mitchell creep model

## 1 Introduction

A large number of large-scale landslides were induced by the coupling effects of rainfall and reservoir water fluctuation in the Three Gorges reservoir area. Under the effects of rainfall and fluctuation of reservoir water, the deformation and long-term stability of these landslides depend on the time-dependent responses of the sliding zone soils significantly. Therefore, it is necessary to carry out creep tests on sliding zone soils of typical landslides in the Three Gorges reservoir area to lay a mechanical foundation for the prediction of long-term stability of these landslides under the influence of reservoir water.

Time-dependent behaviors of soils have been investigated by a number of uniaxial and triaxial tests. Based on these creep testing results, a number of empirical models were proposed, such as Singh-Mitchell creep model [1], Mesri creep model [2], Semple creep model [3], etc. However, there is no creep model explicitly considering the effects of water up to now. In addition, the effect of suction of unsaturated soils on soil properties indicate the effects of water on them [4]. Therefore, it is imperative to establish a suction-related creep model to study the influential mechanism of water on soil creep behavior.

As a typical case, Qianjiangping landslide caused enormous economic loss and social impact. In this paper, a series of unsaturated triaxial creep tests on the sliding zone soils of the Qianjiangping landslide were performed at controlled matric suctions. And an empirical model explicitly considering the effects of matric suction was developed to study the effects of water on the creep behavior of landslide soil quantitatively.

## 2 Unsaturated drained triaxial creep tests

### 2.1 Basic properties of soil samples

The Qianjiangping landslide is located in Zigui Town, Yichang, Hubei Province. It is on the south bank of Qinggan River, a branch of Yangtze River. Soil samples used for laboratory tests were taken from the sliding zone of the Qianjiangping landslide. Then the soil samples were screened through a sieve with a mesh size less than 2 mm to test the basic indices of the soils in laboratory. The results are summarized in Table 1.

Doi: 10.3724/SP.J.1235.2010.00149

*Corresponding author. Tel:+86-15971677316;

E-mail: laixiaoling20031015@yahoo.com.cn

Supported by the National Natural Science Foundation of China (50879044, 50839004)

**Table 1** Physico-mechanical parameters of the sliding zone soils.

| Specific gravity | Water content (%) | Density ($g/cm^3$) | Liquid limit (%) | Plastic limit (%) | Cohesion (kPa) |
|---|---|---|---|---|---|
| 2.71 | 19 | 2.02 | 40.5 | 17 | 28.3 |

In addition, a series of unsaturated triaxial shear tests were performed to determine the unsaturated drained shear strength, $q_f$, for the calculation of shear stress intensity of unsaturated creep tests.

### 2.2 Experimental apparatus and method

The self-developed FSR-6 unsaturated triaxial creep apparatus was employed to conduct the creep tests. It was developed based on the principle of conventional triaxial creep apparatus and unsaturated triaxial apparatus, featuring both the loading system of the former and air pressure controlling system of the latter [5]. Hence, it is available to apply not only constant shear stress but also constant air pressure. The apparatus is composed of several parts, such as confining pressure controlling system, matric suction controlling system, pore water pressure system, axial loading system, cell pressure chamber, measurement and data collecting system, etc. (Fig.1).

(a) The self-developed unsaturated triaxial creep apparatus.

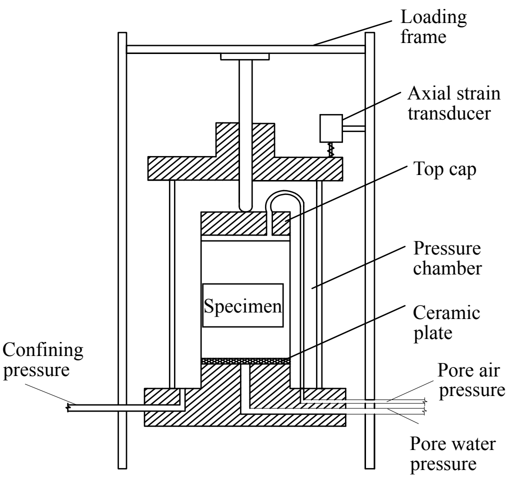


(b) Structure of unsaturated creep apparatus.

**Fig.1** Unsaturated creep apparatus.

The axial load was applied in a conventional way by adopting dead-weights in axial direction. Specimens were cylindrical with a height of 120 mm and a diameter of 60 mm. Drained triaxial creep tests were performed according to the drainage condition of the landslide in a long period of time. Testing process was outlined as follows: (1) Preparation of soil specimens. Remolded samples were prepared in the same way as that in the unsaturated shear tests. Then the specimens were vacuum-saturated. When the measured Skempton *B*-value exceeded 0.95, the samples were considered saturated. (2) Suction equilibrium and consolidation. Prior to consolidation, an air pressure was applied to each specimen to make it reach the suction equilibrium. Then the specimens were consolidated to target confining pressures as shown in Table 2. When the volume of drainage was less than 0.01 $mm^3$ within two hours, consolidation was completed. (3) Creep loading. A deviatonic stress was applied by the multi-stage loading method, which could avoid the inhomogeneity of specimens and obtain more test data in a single creep test. The constant deviatonic stress, $q$, applied at each level of creep was defined as the ratio of the drained shear strength, $q_f$, to the number of loading steps, $n$, i.e. $q= q_f/n$. Specific values of $q$ are summarized in Table 2. It should be noted that the shear strength of specimens was improved due to the multi-stage loading method, hence the drained shear strength, $q_f$, was redefined based on actual creep rupture of tests. If the axial displacement of specimens in each stage of creep was less than 0.01 mm within one day, the creep test in this stage ended and the next level of $q$ was applied until the creep rupture. Thus, the duration of each level of deviatonic stress was 1–2 weeks.

**Table 2** Creep testing program.

| SampleNo. | $\sigma_3$ (kPa) | $u_a$ (kPa) | $\sigma'_3$ (kPa) | $q'_f$ (kPa) | $q_f$ (kPa) | $q$ (kPa) |
|---|---|---|---|---|---|---|
| 1-1 | 150 | 50 | 100 | 176.7 | 182 | 51.5, 103.2, 154.7 |
| 1-2 | 200 | 100 | 100 | 192.1 | 211 | 62.2, 124.7, 182.5 |
| 1-3 | 250 | 150 | 100 | 229.9 | 236 | 70.0, 141.0, 205.0 |
| 2-1 | 300 | 200 | 100 | 267.7 | 340 | 54.9, 109.8, 149.0, 188.2, 227.4, 266.6 |
| 2-2 | 350 | 250 | 100 | 305.5 | 350 | 39.2, 90.2, 141.2, 191.2 |
| 2-3 | 400 | 300 | 100 | 341.2 | 370 | 62.9, 125.8, 188.7, 251.6, 314.5 |

It took nearly one year for three creep apparatuses to complete the unsaturated creep tests in Table 2, and five groups of valid data were obtained. Fitting results of the creep data at a net confining pressure of 100 kPa and a matric suction of 150 kPa are not so good and are absent in this paper. Due to the multi-stage loading method, test data were processed by the principle of Boltzmann superposition. A summary of testing results is illustrated in Table 3, where $\varepsilon_1$ and $\varepsilon_f$ are the axial strains at 60 min and at the end of creep test, respectively; and $t_f$ is the elapsed time. Shear stress intensity, $D_r$, is defined as the ratio of the constant deviatonic stress, $q$, to the drained shear strength, $q_f$, i.e. $D_r = q/q_f$. Figure 2 shows the creep curves at matric suctions of 200, 250 and 300 kPa, respectively.

**Table 3** Summary of creep test results.

| Sample No. | $\sigma_3$ (kPa) | $u_a$ (kPa) | $\sigma_3'$ (kPa) | $D_r$ | $\varepsilon_1$ (%) | $\varepsilon_f$ (%) | $t_f$ (min) |
|---|---|---|---|---|---|---|---|
| 1-1 | 150 | 50 | 100 | 0.283 | 1.65 | 2.23 | 7 203 |
| 1-1 | 150 | 50 | 100 | 0.567 | 4.36 | 5.66 | 11 513 |
| 1-1 | 150 | 50 | 100 | 0.850 | 10.75 | (12.05) | (10.0) |
| 1-2 | 200 | 100 | 100 | 0.295 | 2.34 | 2.69 | 10 727 |
| 1-2 | 200 | 100 | 100 | 0.591 | 4.30 | 5.4 | 11 594 |
| 1-2 | 200 | 100 | 100 | 0.865 | 9.48 | 11.625 | 9 554 |
| 2-1 | 300 | 200 | 100 | 0.161 | 1.94 | 2.41 | 14 748 |
| 2-1 | 300 | 200 | 100 | 0.323 | 2.33 | 3.42 | 21 378 |
| 2-1 | 300 | 200 | 100 | 0.438 | 2.42 | 4.12 | 13 835 |
| 2-1 | 300 | 200 | 100 | 0.553 | 2.73 | 5.34 | 10 727 |
| 2-1 | 300 | 200 | 100 | 0.669 | 3.17 | 6.61 | 9 850 |
| 2-1 | 300 | 200 | 100 | 0.784 | 3.35 | 7.93 | 10 853 |
| 2-2 | 350 | 250 | 100 | 0.112 | 1.88 | 2.77 | 21 375 |
| 2-2 | 350 | 250 | 100 | 0.258 | 2.17 | 3.54 | 13 836 |
| 2-2 | 350 | 250 | 100 | 0.403 | 2.61 | 4.77 | 10 725 |
| 2-2 | 350 | 250 | 100 | 0.546 | 3.23 | 6.27 | 9 849 |
| 2-3 | 400 | 300 | 100 | 0.170 | 1.81 | 2.23 | 14 795 |
| 2-3 | 400 | 300 | 100 | 0.340 | 2.12 | 3.12 | 17 180 |
| 2-3 | 400 | 300 | 100 | 0.510 | 2.25 | 3.95 | 14 060 |
| 2-3 | 400 | 300 | 100 | 0.680 | 2.90 | 5.66 | 10 737 |
| 2-3 | 400 | 300 | 100 | 0.850 | 3.82 | 8.13 | 9 855 |

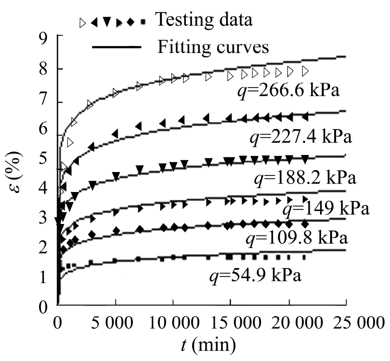


(a) $\sigma_3$ =300 kPa, $u_a$=200 kPa.

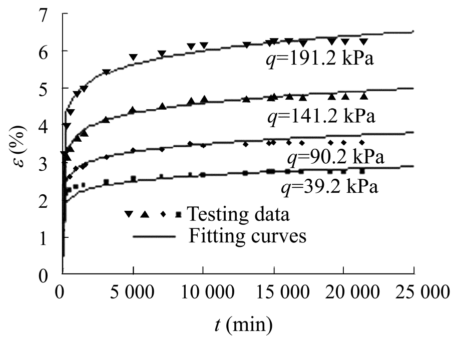


(b) $\sigma_3$ =350 kPa, $u_a$=250 kPa.

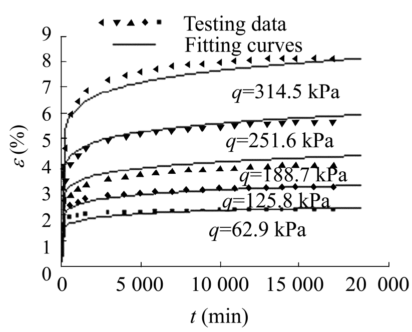


(c) $\sigma_3$ =400 kPa, $u_a$=300 kPa.

**Fig.2** Creep curves of unsaturated triaxial creep tests.

## 3 Unsaturated creep model

### 3.1 Singh-Mitchell stress-strain-time function

The total strain, $\varepsilon$, can be attributed to two components: the instantaneous strain, $\varepsilon_i$, and the time-dependent or creep strain, $\varepsilon_c$, i.e.

$$\varepsilon=\varepsilon_i+\varepsilon_c \tag{1}$$

If a constant stress is applied under undrained condition, $\varepsilon_c$ can be defined as the undrained creep strain. If the stress is applied under drained condition, $\varepsilon_c$ represents the primary consolidation and secondary consolidation (or drained creep). There are many factors affecting the rheological properties of soil, such as overconsolidation ratio, aging, thixotropic effect and temperature. Without consideration of these factors, in general, $\varepsilon_c$ can be approximated by a function of stress and time, i.e.

$$\varepsilon_c=f_1(S)f_2(t) \tag{2}$$

where $f_1(S)$ and $f_2(t)$ denote the functions of stress and time, respectively [6].

**Based on the observation of laboratory creep test results, Singh and Mitchell [1] proposed a creep model that could well describe the creep behavior of soils. In the model, the exponential function and the power function were adopted for $f_1(S)$ and** $f_2(t)$, respectively, i.e.

$$\dot{\varepsilon}=A\exp(\alpha D_r)(t_1/t)^m \tag{3}$$

where $\dot{\varepsilon}$ denotes the axial strain rate at a random time; $t$ is the elapsed time of a creep test; $t_1$ is a referenced time, denoting a time at an early stage of creep test; $A$ is the strain rate at $D_r = 0$, $t = t_1$; $m$ is the inclination of $\ln\dot{\varepsilon}$ versus $\ln t$ plotting; and $\alpha$ is the inclination of $\ln\dot{\varepsilon}$ versus $D_r$ plotting.

Taking natural logarithm on both sides of Eq.(3), it can be rewritten as

$$\ln\dot{\varepsilon}=\ln A+\alpha D_r+m(\ln t-\ln t_1) \tag{4}$$

When $m \neq 1$ and without consideration of initial strain, integrations are performed for Eq.(3), and it can be rewritten as

$$\varepsilon=B\exp(\beta D_r)(t/t_1)^{\lambda} \tag{5}$$

where $B=At_1/(1-m)$, $\beta=\alpha$, and $\lambda=1-m$.

### 3.2 Development of unsaturated creep model

Based on the observation data in the laboratory creep test, it was found that there was a similarity between unsaturated and saturated creep curves. Thus, by using Singh-Mitchell creep model for reference, an unsaturated Singh-Mitchell creep model for the sliding zone soils was attempted to be developed.

**To consider the matric suction as a new stress variable in the unsaturated creep model, a new stress intensity is proposed. As seen in Table 3, the creep strain decreases with the increase in matric suction at a constant net confining pressure, $\sigma_3'$, and stress intensity, $D_r$. Thus, a new stress intensity $D_R$ can be defined as follows:**

$$D_R=D_r\frac{\sigma_3'}{u_a} \tag{6}$$

Substituting Eq.**(6) into Eq.(5),** the unsaturated creep model can be written as

$$\varepsilon=B\exp\left(\beta_{D_R}D_r\frac{\sigma_3'}{u_a}\right)(t/t_1)^{\lambda} \tag{7}$$

where $\beta_{D_R}$ is the corresponding parameter of $\beta$ under the new stress intensity, $D_R$. Taking natural logarithm on both sides of Eq.(7), it can be rewritten as

$$\ln\varepsilon=\ln B+\beta_{D_R}D_R+\lambda(\ln t-\ln t_1) \tag{8}$$

### 3.3 Parameters fitting

The creep curves under a net confining pressure of 100 kPa and a matric suction of 250 kPa were analyzed to describe the developing process of the unsaturated creep model. Let $t_1$ = 60 min, firstly, the $\ln\varepsilon$ versus $\ln t$ plots under different deviatonic stresses are shown in Fig.3.

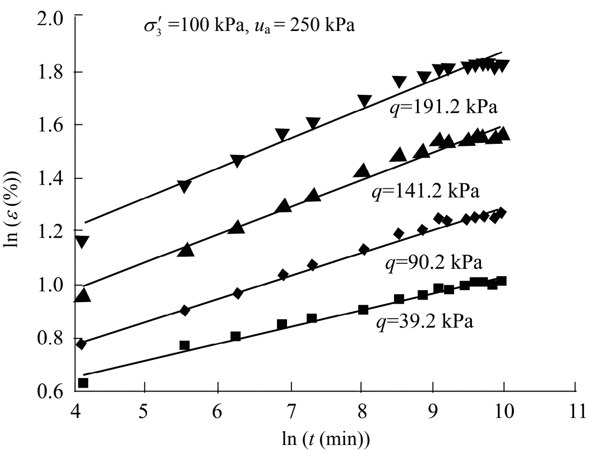


**Fig.3** $\ln t$ - $\ln\varepsilon$ curves.

Clearly, a parallel linear relationship exists between $\ln\varepsilon$ and $\ln t$, and the inclinations of the lines, $\lambda$, under different stress intensities are summarized in Table 4.

**Table 4** Values of $\lambda$ under different stress intensities.

| $q$ (kPa) | $D_r$ | $D_R$ | $\lambda$ | $R^2$ |
|---|---|---|---|---|
| 39.2 | 0.112 | 0.045 | 0.062 7 | 0.984 3 |
| 90.2 | 0.258 | 0.103 | 0.084 7 | 0.987 9 |
| 141.2 | 0.403 | 0.161 | 0.103 1 | 0.982 6 |
| 191.2 | 0.546 | 0.219 | 0.110 2 | 0.971 1 |

Then, $\ln\varepsilon$ versus $D_R$ plots at different elapsed times of 1 500, 5 000, 10 000, 20 000 min are shown in Fig.4. Clearly, a linear relationship exists between $\ln\varepsilon$ and $D_R$, with a slope of $\beta_{D_R}$ and a intercept of $\ln B+\lambda(\ln t-\ln t_1)$. Substituting $\lambda$ and the elapsed time $t_f$ into the intercept formulation, parameter $B$ can then be obtained. Values of $B$ and $\beta_{D_R}$ are summarized in Table 5. As the parameters of Singh-Mitchell model are supposed to be independent of time and stress intensity, average values of these parameters are taken as their final values in the model. Parameters of the unsaturated creep models under five matric suctions are summarized in Table 6, where $\beta$ is the slope of $\ln\varepsilon$ versus $D_r$ plot.

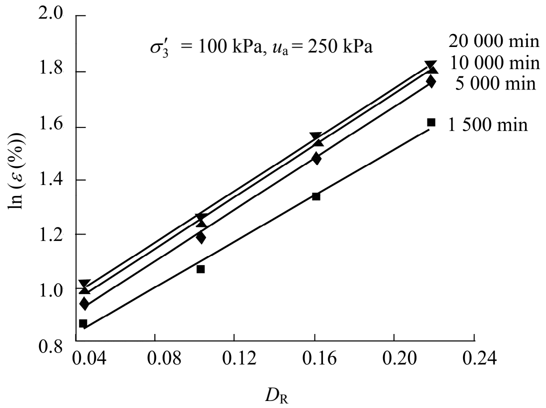


**Fig.4** $D_R$ - ln $\varepsilon$ curves.

**Table 5** Values of $B$ and $\beta$ at different elapsed times.

| $t_f$ (min) | $\beta_{D_R}$ | $B$ | $R^2$ |
|---|---|---|---|
| 1 500 | 4.308 | 1.438 | 0.9 913 |
| 5 000 | 4.766 | 1.376 | 0.9 971 |
| 10 000 | 4.848 | 1.341 | 0.9 979 |
| 20 000 | 4.742 | 1.310 | 0.9 980 |

**Table 6** Parameters used in Singh-Mitchell model.

| $\sigma_3$ (kPa) | $u_a$ (kPa) | $\lambda$ | $\beta_{D_R}$ | $\beta$ | $B$ |
|---|---|---|---|---|---|
| 150 | 50 | 0.045 2 | 1.455 | 2.910 | 0.764 |
| 200 | 100 | 0.036 1 | 2.439 | 2.439 | 1.083 |
| 300 | 200 | 0.087 1 | 3.721 | 1.860 | 1.133 |
| 350 | 250 | 0.090 2 | 4.666 | 1.866 | 1.366 |
| 400 | 300 | 0.090 3 | 6.113 | 1.834 | 1.015 |

Substituting the parameters listed in Table 6 into Eq.(7), we get

$$\left.\begin{aligned}
\varepsilon_1 &= 0.764\exp\left(1.455D_r\frac{\sigma_3'}{u_a}\right)(t/t_1)^{0.045\,2}\\
\varepsilon_2 &= 1.083\exp\left(2.439D_r\frac{\sigma_3'}{u_a}\right)(t/t_1)^{0.036\,1}\\
\varepsilon_3 &= 1.133\exp\left(3.721D_r\frac{\sigma_3'}{u_a}\right)(t/t_1)^{0.087\,1}\\
\varepsilon_4 &= 1.366\exp\left(4.666D_r\frac{\sigma_3'}{u_a}\right)(t/t_1)^{0.090\,2}\\
\varepsilon_5 &= 1.015\exp\left(6.113D_r\frac{\sigma_3'}{u_a}\right)(t/t_1)^{0.090\,3}
\end{aligned}\right\} \tag{9}$$

Equation (9) is the unsaturated Singh-Mitchell creep model of the sliding zone soils of Qianjiangping landslide. Comparison of predicted results using the above models with testing data was conducted for each laboratory test (Fig.2). It is shown that these models can give reasonable predictions of the primary and secondary creeps. But there is a difference when the stress intensity, $D_r$, is high. The calculated creep strain is a little lower than experimental data at early stage of creep and a bit higher at the end of creep. This difference was also been mentioned in Refs.[7, 8]. As for those reasons, some argued that the power function for strain-time relationship in the unsaturated model was not a decay function, while others thought that the parameters of Singh-Mitchell creep model were not independent of time and stress intensity. To deal with this difference, further investigations are needed.

# 4 Analytical results

The effects of matric suction on parameters of Singh-Mitchell creep model were analyzed to further evaluate the influence of suction on the creep characteristics of soil.

(1) Effect of matric suction on $\beta$. $\ln u_a$ versus $\beta$ is plotted in Fig.5. It shows that $\beta$ increases with the

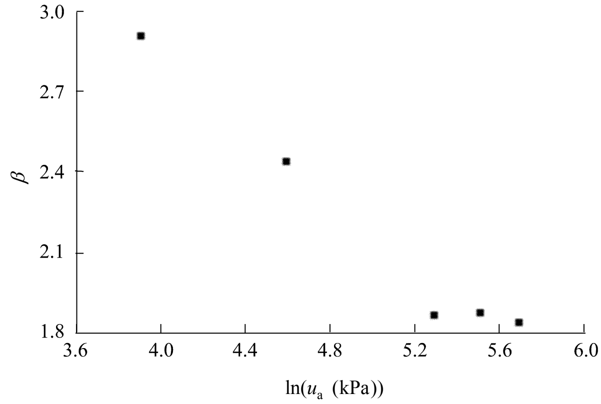


**Fig.5** Relationship between $\beta$ and $\ln u_a$.

decrease in matric suction, which indicates that the amount of creep strain increases with decreasing matric suction at a constant confining pressure and a constant stress intensity.

(2) Effect of matric suction on $\lambda$. Taking into account the discreteness of the samples, $\lambda$ at $\sigma_3 =$ 200 kPa and $u_a =$ 100 kPa is not considered in the plot of $\lambda$ versus $\ln u_a$ (Fig.6). Figure 6 shows that $\lambda$ decreases with the losing of matric suction. Besides, $\lambda = 1 - m$, where $m$ is the slope of $\ln \dot{\varepsilon}$ versus $\ln t$ plot, which reflects the variation rate of creep strain rate. It also indicates that the variation rate of creep strain rate increases due to the decrease in matric suction.

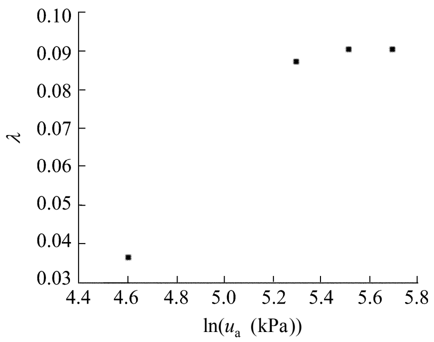


**Fig.6** Relationship between $\lambda$ and $\ln u_a$.

(3) Effect of matric suction on $B$. Relationship between parameter $B$ and $\ln u_a$ is shown in Fig.7. It can be seen that there is some correlation between the two variables, but specific function for them is still difficult to be defined due to a lack of laboratory testing data.

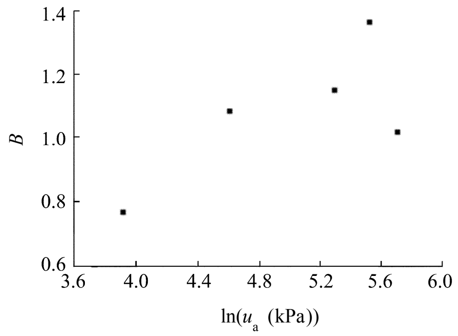


**Fig.7** Relationship between $B$ and $\ln u_a$.

Based on testing results and the above analyses, a conclusion can be drawn that the decrease in matric suction leads to the increase in creep strain rate as well as the amount of creep strain. However, quantitative effects of matric suction on creep strain can still not be defined because of a lack of laboratory data. Thus, much more unsaturated creep tests need to be performed.

# 5 Conclusions

By using the self-developed unsaturated triaxial creep apparatus, two sets of unsaturated creep tests on the sliding zone soils of Qianjiangping landslide were performed. Based on the analyses of testing results, a new stress intensity incorporating matric suction was defined, and a group of unsaturated creep models were presented in this paper. Predicted results are in good agreement with the experimental results.

Analyses of parameters show that the decrease in matric suction leads to reduction in $\lambda$ and increase in $\beta$. This indicates that decrease in matric suction under the influence of water accelerates creep strain rate as well as the amount of creep strain. As long as the correlation between the parameter $B$ and the matric suction is available, quantitative effects of matric suction on creep behavior of soil can be determined. This study provides an insight for the evaluation of long-term stability of the landslide under the influence of water.

Only two sets of unsaturated creep tests were conducted in this paper, and the loading step of each creep test was different, which inevitably brought in some errors. However, because the relationship between the parameter $B$ and the matric suction is not defined, more unsaturated creep tests need to be conducted to further investigate and improve the unsaturated creep model.

## References

[1] Singh A, Mitchell J K. General stress-strain-time function for soils. Journal of Soil Mechanics and Found Engineering Division, ASCE, 1968, 94 (1): 21–46.

[2] Mesri G. Febres-Cordero E, Shields D R, et al. Shear stress-strain-time behavior of clays. Geotechnique, 1981, 31 (4): 537–552.

[3] Semple R M. The effect of time-dependent properties of altered rock on the tunnel support requirements. PhD Thesis. Urbana: University of Illinois, 1973.

[4] Fredlund D G, Rahardjo H. Soil mechanics for unsaturated soil. Beijing: China Architecture and Building Press, 1997 (in Chinese).

[5] Guan Ni, Wang Shimei. Discussion on creep test methods of unsaturated soil. Journal of Three Gorges University (Natural Sciences), 2008, 30 (2): 32–34 (in Chinese).

[6] Lin H D, Wang C C. Stress-strain-time function of clay. Journal of Geotechnical and Geoenvironmental Engineering, 1998, 124 (4): 289–296.

[7] Wang Chen, Zhang Yongli, Liu Haowu. A modified Singh-Mitchell's creep function of sliding zone soils of Xietan landslide in the Three Gorges. Rock and Soil Mechanics, 2005, 26 (3): 415–418 (in Chinese).

[8] Lu Pingzhen, Zeng Jing, Sheng Qian. Creep tests on soft clay and its empirical models. Rock and Soil Mechanics, 2008, 29 (4): 1 041– 1 044 (in Chinese).